

Light Impulsive Damping of Spacecraft Exhibiting Normal Mode Behavior

Larry Silverberg*

North Carolina State University, Raleigh, North Carolina 27695

This paper develops an impulsive damping control algorithm suitable for spacecraft. The fuel optimal solutions to the problem of damping the motion of spacecraft consists of impulsive control forces applied at repeated instances in time. The instances in time occur when the spacecraft undergoes maximum absolute velocities and minimum absolute displacements. This paper approximates impulses by short duration pulses. Maximum absolute velocities and minimum absolute displacements are then approximated by transient values of their respective standard deviations. Impulsive damping is achieved by applying either a large single pulse or smaller repeated pulses. A near fuel optimal mode preserving impulsive damping control algorithm is developed next. The algorithm exhibits the following properties: 1) the impulsive damping control algorithm is independent of spacecraft stiffness, 2) the associated control forces are proportional to spacecraft inertia, and 3) the impulsive damping control algorithm is decentralized. The impulsive damping of a cantilever beam demonstrates the results.

I. Introduction

IMPULSIVE forces are used to propel spacecraft in a fuel optimal manner. For example, the fuel optimal problem of transferring a spacecraft between two coplanar circular orbits, first solved by Hohmann in 1925, requires a pair of impulses. As another example, fuel optimal thrusting maneuvers of satellites are carried out by multiple impulses (see Ref. 1 describing fuel optimal maneuvers of the Space Shuttle Orbiter). Similarly, impulsive forces provide the fuel optimal solution to the problem of damping the motion of flexible spacecraft.

A concise formulation of fuel-optimal control was developed by Neustadt in 1962.² In contrast with linear optimal control, in which a pseudofuel function of the form

$$\int_0^T f^2(t) dt$$

is minimized, fuel optimal control minimizes the absolute fuel function of the form

$$\int_0^T |f(t)| dt$$

where $f(t)$ denotes the control force at time t over the time interval $[0, T]$. The minimization of absolute fuel admits impulsive control forces, whereas the minimization of pseudofuel does not allow for impulsive forces. Linear optimal control cannot admit impulsive control forces since the unit impulse at time t_0 given by $f(t) = \delta(t - t_0)$ consumes an infinite amount of pseudofuel, that is,

$$\int_0^T \delta^2(t - t_0) dt = \infty$$

To better appreciate why fuel optimal control problems admit impulsive forces, consider the linear harmonic oscillator (of unit mass). The energy in the oscillator at time t is given by

$$E(t) = \frac{1}{2} \dot{q}^2(t) + \frac{1}{2} \omega^2 q^2(t)$$

in which the first term is recognized as kinetic energy and the second term is recognized as potential energy where $q(t)$ denotes displacement and ω denotes natural frequency of oscillation. The work performed by the control force $Q(t)$ over the control time T is given by

$$W = \int_0^T Q(t) \dot{q}(t) dt$$

The control force can be expressed as an integral of infinitesimal impulses, and since the oscillator is linear, by superposition the displacement can be expressed as an integral of associated impulse responses. This is commonly known as the convolution theorem. It follows in seeking a fuel optimal control that we can first examine the associated impulse responses and then superimpose the results.

The work performed by the unit impulse at time t_0 denoted by $Q(t) = \delta(t - t_0)$ where $0 < t_0 < T$ and the associated change in energy over the control time T are both identical to

$$E(T) - E(0) = W = \frac{1}{2} + \dot{q}(t_0^-)$$

in which t_0^- denotes the time just before the applied impulse. The corresponding amount of fuel consumed, given by

$$Fu = \int_0^T |Q(t)| dt$$

is unity. Indeed, a unit amount of fuel causes a change in the oscillator's energy that is proportional to the oscillator's velocity (Fig. 1). Our interest lies in reducing the oscillator's energy to zero. Therefore, an impulse applied at the instant the oscillator undergoes its maximum absolute velocity and in the opposite direction will cause the greatest reduction in energy for a fixed amount of fuel. Furthermore, the oscillator's maximum absolute velocity occurs when its displacement is identically zero. Therefore, by superposition, the control force has the form of an impulse function applied at an instant of maximum absolute velocity and minimum absolute dis-

Received July 2, 1990; revision received Dec. 3, 1990; accepted for publication Jan. 23, 1991. Copyright © 1991 by Larry Silverberg. Published by the American Institute of Aeronautics and Astronautics, Inc., with permission.

*Associate Professor, Mars Mission Research Center, Department of Mechanical Engineering, Box 7910. Member AIAA.

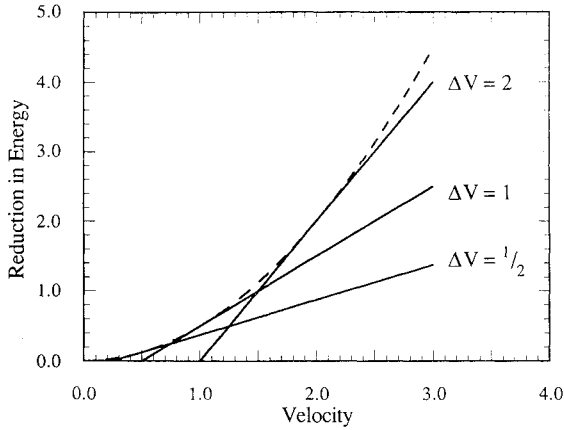


Fig. 1 Reduction in oscillator energy $E(t^-) - E(t^+)$ vs oscillator velocity $\dot{q}(t^-)$ for different impulses.

placement. This form of control is referred to here as the impulse principle.

The impulse principle just described for the harmonic oscillator also applies to spacecraft exhibiting normal mode behavior.^{3,4} Recognizing that the vibration of spacecraft can be modeled as a linear combination of harmonic oscillators, the fuel optimal spacecraft control forces based on such a model have the form of a combination of impulses applied at instances of maximum absolute velocities and minimum absolute displacements.

Section II reviews impulsive damping of a harmonic oscillator. Statistical approximations of spacecraft maximum absolute velocities and minimum absolute displacements are developed in Sec. III. These approximations provide the computational means of implementing impulsive damping algorithms. On the basis of the previously indicated statistical approximations, the impulsive control forces are modified in Sec. IV. Next, a near fuel optimal impulsive damping control algorithm is developed in Sec. V for flexible spacecraft. The associated control parameters are computed based on results obtained for the harmonic oscillator. Impulsive damping of a cantilever beam is considered in Sec. VI.

II. Impulsive Damping of a Harmonic Oscillator

The undamped harmonic oscillator (of unit mass) is governed by the differential equation of motion

$$\ddot{q}(t) + \omega^2 q(t) = Q(t) \quad (1)$$

where $q(t)$ denotes the displacement at time t , $Q(t)$ denotes the control force, and ω denotes the natural frequency of oscillation. The fuel optimal control problem is formulated as a two-point boundary value problem in which we minimize the absolute fuel

$$Fu = \int_0^T |Q(t)| dt \quad (2)$$

subject to the equation of motion [Eq. (1)] and the prescribed boundary conditions at the initial and final times

$$q(0) = q_0, \quad \dot{q}(0) = \dot{q}_0, \quad q(T) = q_1, \quad \dot{q}(T) = \dot{q}_1$$

The interest is to bring the oscillator to rest in control time T , and so we let $q_1 = \dot{q}_1 = 0$. The fuel optimal control force is given by^{2,5}

$$Q(t) = -Q_0(t) \operatorname{sgn} \dot{q}(t) \quad (3)$$

where

$$\max_{0 \leq s \leq T} |\dot{q}(s)| = |\dot{q}(t_0)| \quad (4a)$$

$$Q_0(t) = |\dot{q}(t_0)| \delta(t - t_0) \quad (4b)$$

Furthermore, note that

$$\min_{0 \leq s \leq T} |q(s)| = |q(t_0)| = 0 \quad (5)$$

As indicated by Eqs. (3) and (4), the fuel optimal control force is an impulse function applied at the instant the oscillator undergoes its maximum absolute velocity. The magnitude of the impulse is identical to the oscillator's maximum absolute velocity, and the impulse acts in the opposite direction of the oscillator velocity. As indicated by Eq. (5), the minimum absolute displacement and maximum absolute velocity occur simultaneously at time t_0 , and the minimum absolute displacement is identically zero.

Additional characteristics associated with the fuel optimal control force depend on the control time T . When

$$T < \frac{1}{\omega} \left(\frac{\pi}{2} - \tan^{-1} \left| \frac{\dot{q}_0}{\omega q_0} \right| \right)$$

in which

$$0 \leq \tan^{-1} \left| \frac{\dot{q}_0}{\omega q_0} \right| \leq \frac{\pi}{2}$$

the harmonic oscillator will not be controlled by impulse functions. Letting $\dot{q}_0 = 0$, the harmonic oscillator is not controlled by impulse functions when $T < \pi/2\omega$. When $\pi/2\omega \leq T < \pi/\omega$, the time t_0 in Eqs. (4) is single valued, taking on the value $t_0 = \pi/2\omega$. When $\pi/2\omega \leq T < (n+1)\pi/2\omega$, for $n > 1$, the time t_0 is multivalued, taking on the values $t_{0r} = r\pi/2\omega$, ($r = 2, 3, \dots, n$). The magnitudes of the impulses applied at each t_{0r} , ($r = 2, 3, \dots, n$), are arbitrarily distributed. The impulses in Eq. (3) are then expressed as

$$Q_0(t) = \sum_{r=1}^n |Q_{0r}| \delta(t - t_{0r}) \quad (6a)$$

$$\sum_{r=1}^n |Q_{0r}| = |\dot{q}(t_{01})| \quad (6b)$$

in which Q_{0r} denotes the magnitude of the impulse applied at t_{0r} .

The nature of the fuel optimal control force, described here within the context of controlling the motion of a harmonic oscillator, is preserved as we extend our context to controlling the motion of spacecraft exhibiting normal mode behavior. These characteristics associated with the fuel optimal control force are referred to in this paper as the impulse principle.

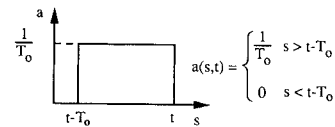


Fig. 2a Rectangular window.

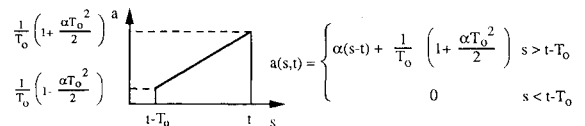


Fig. 2b Linear window.

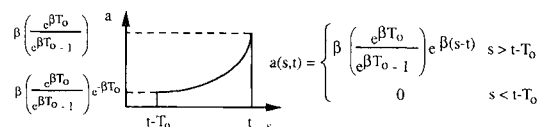
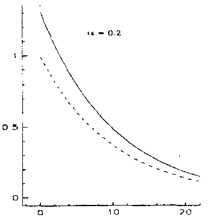
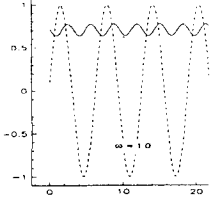
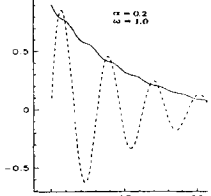
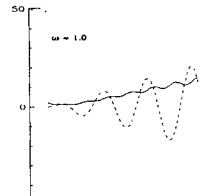


Fig. 2c Exponential window.

Table 1 Transient values of the standard deviation of $f(t)$ based on a rectangular window

$f(t)$	$\sigma_f^2(t) = \frac{1}{T} \int_{t-T}^t f^2(s) ds$	
$e^{-\alpha t}$	$\left(-\frac{1}{2\alpha T}\right)e^{-2\alpha t}(1 - e^{2\alpha T})$	$\sigma_f(t)$: solid line $f(t)$: dashed line
$\sin(\omega t)$	$(1/2) \left[1 - \left(\frac{1}{2\omega T}\right) \{\sin 2\omega t - \sin 2\omega(t-T)\} \right]$	
$\cos(\omega t)$	$(1/2) \left[1 + \left(\frac{1}{2\omega T}\right) \{\sin 2\omega t - \sin 2\omega(t-T)\} \right]$	
$e^{-\alpha t} \sin(\omega t)$	$(1/T) \left[\left(\frac{1}{4\omega^2 + 4\alpha^2}\right) \left\{ (-2\alpha \sin \omega t - 2\omega \cos \omega t)e^{-2\alpha t} \sin \omega t + \left(\frac{\omega^2}{\alpha}\right)(e^{-2\alpha T} - e^{-2\alpha t}) + (2\alpha \sin \omega T + 2\omega \cos \omega T)e^{-2\alpha T} \sin \omega T \right\} \right]$	
$e^{-\alpha t} \cos(\omega t)$	$(1/T) \left[\left(\frac{1}{4\omega^2 + 4\alpha^2}\right) \left\{ (-2\alpha \cos \omega t - 2\omega \sin \omega t)e^{-2\alpha t} \cos \omega t + \left(\frac{\omega^2}{\alpha}\right)(e^{-2\alpha T} - e^{-2\alpha t}) + (2\alpha \cos \omega T + 2\omega \sin \omega T)e^{-2\alpha T} \sin \omega T \right\} \right]$	
$(t) \sin(\omega t)$	$(1/T) \left\{ t^3/6 - \left(\frac{t^2}{4\omega} - \frac{1}{8\omega^3}\right) \sin 2\omega t - (t \cos 2\omega t)/4\omega^2 - (t-T)^3/6 + \left[\frac{(t-T)^2}{4\omega} - \frac{1}{8\omega^3}\right] \sin 2\omega(t-T) + [(t-T) \cos 2\omega(t-T)]/4\omega^2 \right\}$	
$(t) \cos(\omega t)$	$(1/T) \left\{ t^3/6 - \left(\frac{t^2}{4\omega} - \frac{1}{8\omega^3}\right) \sin 2\omega t - (t \cos 2\omega t)/4\omega^2 - (t-T)^3/6 + \left[\frac{(t-T)^2}{4\omega} - \frac{1}{8\omega^3}\right] \sin 2\omega(t-T) + [(t-T) \cos 2\omega(t-T)]/4\omega^2 \right\}$	

The fuel optimal control force given by Eqs. (3-5) is now rewritten in the statistical form

$$Q(t) = \begin{cases} -Q_0(t) \operatorname{sgn} \dot{q}(t) & E_1 \cap E_2 \\ 0 & \text{otherwise} \end{cases} \quad (7)$$

where

$$E_1 = \{t: |\dot{q}(t)| \geq \max_{0 \leq s \leq T} |\dot{q}(s)|\} \quad (8a)$$

$$E_2 = \{t: |q(t)| \leq \min_{0 \leq s \leq T} |q(s)|\} \quad (8b)$$

in which the event E_1 corresponds to the times t in which the absolute velocity is greater than or equal to the maximum absolute velocity over the control time T , and the event E_2 corresponds to the times t in which the absolute displacement is less than or equal to the minimum absolute displacement over the control time T . Of course, both events E_1 and E_2 and, hence, $E_1 \cap E_2$ occur when $t = t_0$. Therefore, in the case of a harmonic oscillator E_1 , E_2 and $E_1 \cap E_2$ are equivalent. The statistical form given by Eqs. (7) and (8) will be used later to replace the events E_1 and E_2 with statistical approximations of these events. Furthermore, this statistical form of the control force will be used as we extend the result from the harmonic oscillator to spacecraft exhibiting normal mode behavior.

III. Statistical Approximations of Maximum Absolute Velocity and Minimum Absolute Displacement

In practice, an impulse applied at a single point in time is replaced by a pulse applied over a small pulse time. The question arises concerning how to determine the magnitude of the pulse, the pulse time, the maximum absolute velocity, and the minimum absolute displacement. The answer to this question is provided by transient values of standard deviations of displacement and velocity. Letting $f(t)$ represent either a displacement or a velocity at time t , we write

$$\sigma_f^2(t) = \int_{t-T_0}^t a(t-s)f^2(s) ds \quad (9a)$$

$$\int_0^{T_0} a(\xi) d\xi = 1 \quad (9b)$$

in which $\sigma_f(t)$ denotes the weighted standard deviation of $f(t)$ at time t , $a(\xi)$ denotes a window shape, and T_0 denotes a window time. Different weighting functions or windows are shown in Fig. 2. Transient values of the standard deviation of $f(t)$ based on the rectangular window are given in Table 1. Steady-state values of standard deviations are represented by

$$\sigma_f^\infty = \lim_{t, T_0 \rightarrow \infty} \sigma_f(t)$$

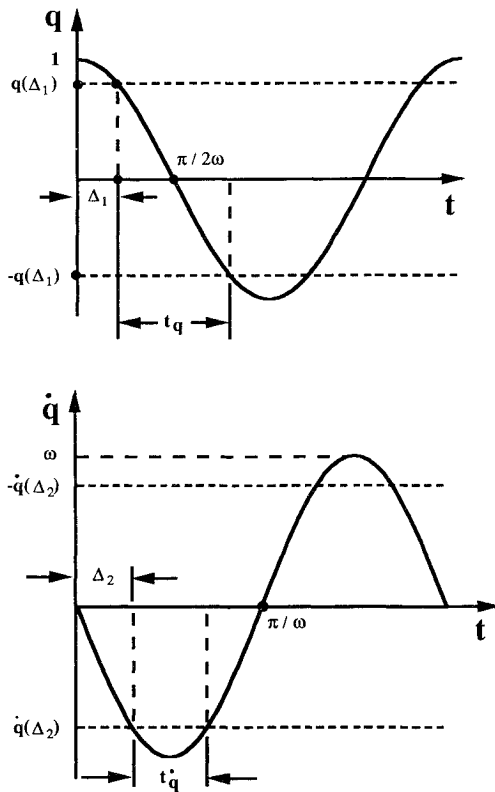


Fig. 3 Pulse times of a harmonic oscillator.

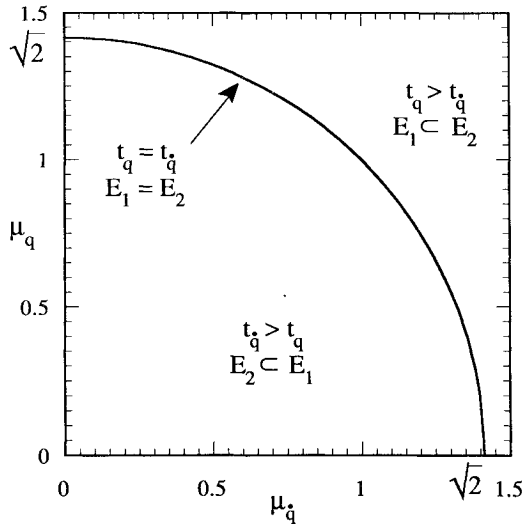
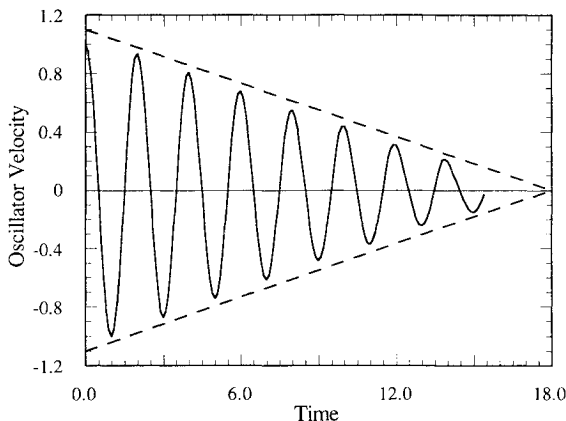
Fig. 4 Selection of control gains μ_q and $\mu_{\dot{q}}$.

Fig. 5 Oscillator velocity.

The steady-state values of the standard deviations of $\sin(\omega t)$ and $\cos(\omega t)$ in Table 1 are identically $\sqrt{2}/2$. The recursive form associated with Eqs. (9) is obtained by differentiating Eqs. (9) with respect to time to get

$$\frac{d\sigma_f^2(t)}{dt^2} = \int_{t-T_0}^t \frac{\partial a(t-s)}{\partial t} f^2(s) ds + a(0)f^2(t) - a(T_0)f^2(t-T) \quad (10)$$

Equation (10) can be simplified depending on the shape of the window. In the case of a rectangular window, $[\partial a(t-s)]/\partial t = 0$, in the case of a linear window, $[\partial a(t-s)]/\partial t = \alpha$, and in the case of an exponential window, $[\partial a(t-s)]/\partial t = \alpha a(t-s)$. The associated pulse times are determined throughout the remainder of the paper using the recursive form of the standard deviation given in Eq. (10). Furthermore, although the use of the linear and exponential windows adequately determines the indicated pulse times, for simplicity, we shall from now on restrict our attention to the rectangular window.

IV. Modification of the Impulsive Control Force

The impulsive control force is now modified by replacing an impulse applied at a point in time with a finite pulse applied over a short pulse time. We first express the maximum absolute velocity and the minimum absolute displacement in Eqs. (8) in terms of the steady-state values of the associated standard deviations multiplied by appropriate control gains. We write

$$\max_{0 \leq s \leq T} |\dot{q}(s)| = \mu_{\dot{q}} \sigma_{\dot{q}}^\infty \quad (11a)$$

$$\min_{0 \leq s \leq T} |q(s)| = \mu_q \sigma_q^\infty \quad (11b)$$

where $\mu_{\dot{q}}$ and μ_q are control gains. Since $q(t)$ and $\dot{q}(t)$ are harmonic functions, it follows that $\mu_{\dot{q}} = \sqrt{2}$ and $\mu_q = 0$. The impulsive control force is now modified by approximating steady-state values of standard deviations by transient values of standard deviations. Transient values of standard deviations closely approximate steady-state values of standard deviations when $\omega T_0 \gg 1$. Substituting the modified Eqs. (11) into Eqs. (8), we obtain the modified events

$$E_1 = \{t: |\dot{q}(t)| \geq \mu_{\dot{q}} \sigma_{\dot{q}}(t)\} \quad (12a)$$

$$E_2 = \{t: |q(t)| \leq \mu_q \sigma_q(t)\} \quad (12b)$$

The impulse function is approximated by a finite pulse acting over a pulse time t_p . The pulse time depends on the control gains $\mu_{\dot{q}}$ and μ_q in Eqs. (12). The pulse time associated with event E_1 increases as $\mu_{\dot{q}}$ decreases below $\sqrt{2}$. Likewise, the pulse time associated with event E_2 increases as μ_q increases above zero. The pulse times are obtained as follows. Without loss of generality, consider initial conditions $q(0) = 1$ and $\dot{q}(0) = 0$. With these initial conditions, the harmonic oscillator would receive an impulse at time $t = \pi/2\omega$. Instead, the harmonic oscillator receives a pulse of duration t_q associated with event E_1 in Eq. (12a) and of duration $t_{\dot{q}}$ associated with event E_2 in Eq. (12b). By approximating transient values of standard deviations as their associated steady-state values, we see from Fig. 3 that

$$q(\Delta_1) = \cos\left(\frac{\pi}{2\omega} - \frac{t_q}{2}\right) \quad (13a)$$

$$\dot{q}(\Delta_2) = \omega \sin\left(\frac{1}{2}\left(\frac{\pi}{\omega} - t_q\right)\right) \quad (13b)$$

where t_q denotes the pulse time associated with event E_1 and $t_{\dot{q}}$ denotes the pulse time associated with event E_2 . Furthermore, from Fig. 3,

$$\mu_q \sigma_q^\infty = q(\Delta_1) \quad (14a)$$

$$\mu_q \sigma_q^\infty = \dot{q}(\Delta_2) \quad (14b)$$

Substituting Eqs. (14) into Eqs. (13), we obtain the pulse times for events E_1 and E_2

$$t_q = \frac{2}{\omega} \sin^{-1} \left(\frac{\mu_q}{\sqrt{2}} \right) \quad (15a)$$

$$t_q = \frac{2}{\omega} \cos^{-1} \left(\frac{\mu_q}{\sqrt{2}} \right) \quad (15b)$$

Equations (15) accurately approximate the pulse times for E_1 and E_2 in Eqs. (12) when $\omega t_q \ll 1$ and when $\omega t_q \gg 1$, respectively. When $t_q > t_q$, then event E_2 becomes a passive constraint since $E_1 \cap E_2 = E_1$ in Eq. (7). Similarly, when $t_q < t_q$, then event E_1 becomes a passive constraint since $E_1 \cap E_2 = E_2$ in Eq. (7). Passive constraints are avoided by selecting identical pulse times for E_1 and E_2 . Under these conditions, we obtain the pulse time

$$t_p = t_q = t_q \quad (16)$$

Substituting Eq. (16) into Eqs. (15), we obtain the control gain constraint equation (see Fig. 4)

$$0 = \mu_q^2 + \mu_q^2 - 4 \quad (17)$$

As shown, event E_1 is an active constraint below the constraint curve in which E_1 guarantees fuel optimal pulse times. Event E_2 is an active constraint above the constraint curve in which E_2 further guarantees fuel optimal pulse times.

Single Impulsive Damping

The single impulse function in Eqs. (3) and (7) is now approximated by

$$Q_0(t) = |\dot{q}(t)|\beta \quad (18a)$$

$$\beta t_p = 1 \quad (18b)$$

Substituting Eqs. (18) into Eq. (7), approximating Eqs. (8) by Eqs. (12), we obtain the single impulsive damping control algorithm

$$Q(t) = \begin{cases} -\beta \dot{q}(t) & E_1 \cap E_2 \\ 0 & \text{otherwise} \end{cases} \quad (19)$$

where

$$E_1 = \{t: |\dot{q}(t)| \geq \mu_q \sigma_q(t)\}, \quad E_2 = \{t: |q(t)| \leq \mu_q \sigma_q(t)\}$$

Uniformly Distributed Impulsive Damping

Rather than apply a single pulse, multiple pulses of smaller magnitudes can be applied as indicated by Eqs. (6). Consider a uniform distribution of pulses. We replace Eqs. (18) with

$$Q_0(t) = Q_0 \quad (20a)$$

$$Q_0 t_p \ll \dot{q}_0 \quad (20b)$$

By substituting Eqs. (20) into Eq. (7) and approximating Eqs. (8) by Eqs. (12), we obtain the uniformly distributed impulsive damping algorithm

$$Q(t) = \begin{cases} -Q_0 \operatorname{sgn} \dot{q}(t) & E_1 \cap E_2 \\ 0 & \text{otherwise} \end{cases} \quad (21)$$

where

$$E_1 = \{t: |\dot{q}(t)| \geq \mu_q \sigma_q(t)\}, \quad E_2 = \{t: |q(t)| \leq \mu_q \sigma_q(t)\}$$

Under these conditions, a constant pulse is applied approximately every half period and the change in velocity due to each pulse is $Q_0 t_p$. From Eqs. (15) and (16), we obtain the linear decay rate associated with the oscillator velocity

$$\gamma = \frac{2\sqrt{2}}{\pi} Q_0 \mu_q \quad (22)$$

From Eq. (22), the linear decay rate γ is independent of the oscillator's natural frequency of oscillation (see Fig. 5).

V. Light Impulsive Damping of Spacecraft Exhibiting Normal Mode Behavior

We assume that the spacecraft is governed by the partial differential equation

$$m(x) \frac{\partial^2 u(x,t)}{\partial t^2} = -Tu(x,t) + f(x,t) \quad (23)$$

where $m(x)$ denotes mass distribution, $u(x,t)$ denotes displacement, $f(x,t)$ denotes control force distribution, and T represents an appropriate linear stiffness operator. The stiffness operator is self-adjoint and positive (semi-) definite, implying that the spacecraft exhibits normal mode behavior.⁹ Under these conditions, the spacecraft is regarded as a linear combination of harmonic oscillators. The displacement and force are expressed as the linear combinations

$$u(x,t) = \sum_{r=1}^{\infty} \phi_r(x) q_r(t) \quad (24a)$$

$$q_r(t) = \int_D m(x) \phi_r(x) u(x,t) dx$$

$$f(x,t) = m(x) \sum_{r=1}^{\infty} \phi_r(x) Q_r(t) \quad (24b)$$

$$Q_r(t) = \int_D \phi_r(x) f(x,t) dx$$

where $\phi_r(x)$ denotes the r th natural mode of vibration and the integration is carried out over the domain D of the spacecraft.

Single Mode Participation

The relationship between impulsive damping of spacecraft and impulsive damping of a harmonic oscillator is brought out by first considering the participation of a single mode of vibration in the system response and by considering the distributed (in space) control force that excites this mode. Thus,

$$u(x,t) = \phi_s(x) q_s(t) \quad (25a)$$

$$f(x,t) = m(x) \phi_s(x) Q_s(t) \quad (25b)$$

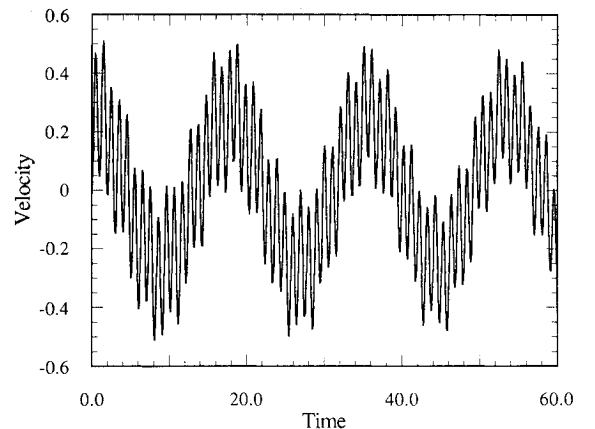


Fig. 6 Free tip response.

Substituting Eqs. (25) into Eq. (19), we obtain the associated impulsive damping control algorithm

$$f(x, t) = \begin{cases} -\beta m(x) \dot{u}(x, t) & E_1 \cap E_2 \\ 0 & \text{otherwise} \end{cases} \quad (26)$$

where

$$E_1 = \{t: |\dot{u}(x, t)| \geq \mu_{ii} \sigma_{ii}(t)\} \quad (27a)$$

$$E_2 = \{t: |u(x, t)| \leq \mu_{ii} \sigma_{ii}(t)\} \quad (27b)$$

Letting

$$\mu_{ii}(x, t) = \mu_{ij} \quad (28a)$$

$$\mu_{ii}(x, t) = \mu_{ij} \quad (28b)$$

Eqs. (27) become identical to Eq. (19). Next, by letting

$$\mu_{ij} = \sqrt{2}, \quad \mu_{ij} = 0, \quad \beta = \delta(t - t_0) \quad (29)$$

where t_0 is the instant in time corresponding to the maximum absolute velocity, the spacecraft motion is damped out by a single spatially distributed impulse. Furthermore, we learn from Eqs. (28) that the spacecraft control gains in Eqs. (28) are identical to the control gains for the harmonic oscillator.

Mode Preserving Distributed Control Forces

In the presence of the participation of a multiple number of modes of vibration, the control law given by Eq. (26) preserves the natural modes of vibration; that is, the closed-loop modes of vibration are identical to the natural modes of vibration. The preservation of the natural modes of vibration is a property of fuel optimal control.⁶ The natural modes of vibration are preserved only if the control force does not recouple the associated modal equations of motion. Thus, the preservation of the natural modes of vibration is verified by substituting Eq. (26) into Eqs. (24) to obtain

$$Q_r(t) = \begin{cases} -\beta \dot{q}_r(t) & E_1 \cap E_2 \\ 0 & \text{otherwise} \end{cases} \quad (30)$$

From Eq. (30), the r th modal force depends on $\dot{q}_r(t)$ and no other modal coordinates from which it follows that Eq. (26) is a mode preserving control. Note, however, that E_1 and E_2 do not separate by mode. The use of distributed forces, as indicated by Eq. (26), is frequently beyond the current state of the art.

Mode Preserving Discrete Control Forces

Discrete forces are expressed in terms of a distributed force as

$$f(x, t) = \sum_{r=1}^n F_r(t) \delta(x - x_r) \quad (31)$$

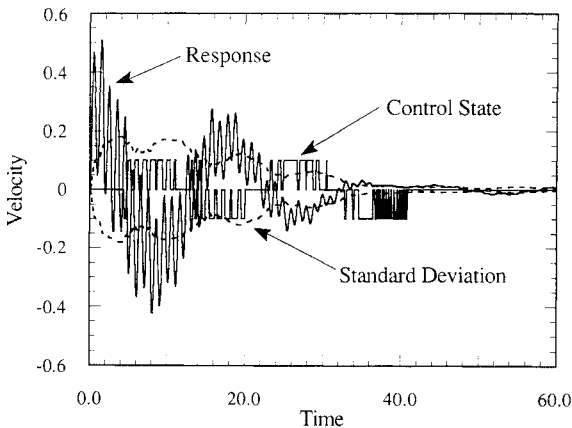


Fig. 7 Controlled tip response: $\mu_q = 1.4213$; $\mu_{ij} = 0.70$; $T_0 = 4$ s.

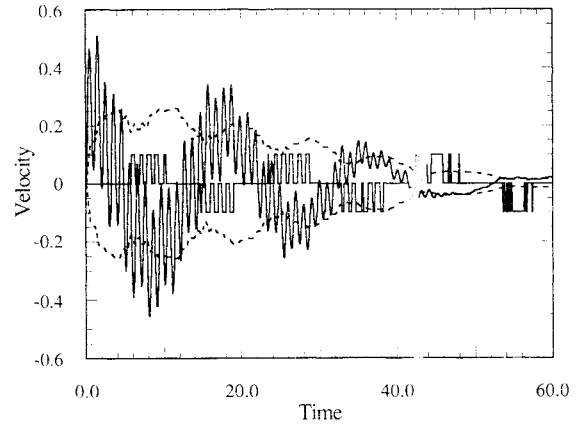


Fig. 8 Controlled tip response: $\mu_q = 1.0824$; $\mu_{ij} = 1.00$; $T_0 = 4$ s.

where $F_r(t)$ ($r = 1, 2, \dots, n$) denote discrete forces located at x_r ($r = 1, 2, \dots, n$), respectively. The control law given by Eq. (26) is now approximated using discrete forces. Toward this end, the spacecraft is divided into subdomains, each containing a discrete control force at its mass center.⁷ Integrating Eq. (26) over each subdomain, we obtain

$$F_r(t) = \int_{D_r} f(x, t) dx = \begin{cases} -\beta \int_{D_r} m \dot{u} dx & E_1 \cap E_2 \\ 0 & \text{otherwise} \end{cases} \quad (32)$$

where D_r denotes the r th subdomain. The displacement in each subdomain is approximated by a two-term truncated Taylor series approximation about the mass center, given by

$$u = u(x_r, t) + \left. \frac{\partial u}{\partial x} \right|_{x=x_r} (x - x_r), \quad (r = 1, 2, \dots, n) \quad (33)$$

The two terms retained in the Taylor series are associated with the rigid-body components of the motion in the subdomain, whereas the remaining neglected terms are associated with the flexible-body components of the motion in the subdomain. Substituting Eq. (33) into Eq. (32), and considering the identity

$$\int_{D_r} m(x - x_r) dx = 1$$

which follows from the definition of a mass center, we obtain the single impulsive damping algorithm

$$F_r(t) = \begin{cases} -\beta m_r \dot{u}(x_r, t) & E_1 \cap E_2 \text{ at } x = x_r \\ 0 & \text{otherwise} \end{cases} \quad (34)$$

where

$$m_r = \int_{D_r} m dx, \quad (r = 1, 2, \dots, n)$$

denotes the mass of the r th subdomain and where we recall that $\beta t_p = 1$. The discrete control forces described by Eq. (34) approximate the distributed force described by Eq. (26). The errors introduced in the approximation cause errors in the response of the spacecraft at the control time T ; that is, the motion of the spacecraft is only approximately driven to zero in control time T .

Uniformly Distributed Impulsive Damping Using Discrete Control Forces

Rather than apply large discrete pulses at one instant in time, discrete pulses of smaller magnitudes can be applied repeatedly. Consider uniformly distributed pulses (in time), and let the spatial distribution of the discrete pulses (in space) be proportional to the mass distribution. We obtain from Eq. (34) the impulsive damping control algorithm for the spacecraft

$$F_r(t) = \begin{cases} -\beta m_r \operatorname{sgn} \dot{u}(x_r, t) & E_1 \cap E_2 \text{ at } x = x_r \\ 0 & \text{otherwise} \end{cases} \quad (35)$$

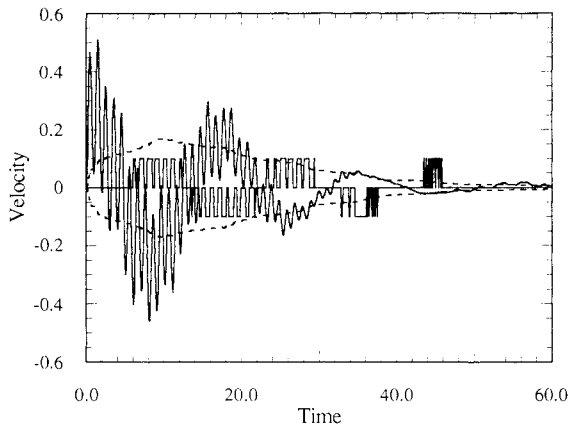


Fig. 9 Controlled tip response: $\mu_q = 1.4213$; $\mu_q = 0.70$; $T_0 = 10$ s.

where the spatial distribution of $\text{sgn } \dot{u}(x_r, t)$ in Eq. (35) can be regarded as an approximation of the spatial distribution of $\dot{u}(x_r, t)$ in Eq. (34).

The β parameter in Eq. (35) influences the rate of decay of the spacecraft motion. The rate of decay of the motion is approximated by temporarily reconsidering single mode participation of the s th mode [Eq. (25)]. Substituting Eqs. (35), (25), and (31) into Eqs. (24), we obtain the r th modal control force

$$Q_r(t) = -\beta \sum_{s=1}^n c_{rs} \text{sgn } q_s(t) \quad (36a)$$

$$c_{rs} = \sum_{i=1}^n \phi_r(x_i) \text{sgn } \phi_s(x_i) m_i \quad (36b)$$

where c_{rs} are coupling coefficients.⁸ The coupling coefficients can approximate the Kronecker delta function, that is, $c_{rs} \approx \delta_{rs}$, where $\delta_{rr} = 1$ and $\delta_{rs} = 0$ for $r \neq s$. Note that the diagonalization of the coupling coefficients provides a fuel optimal basis for the optimal selection of the locations of the control forces and of the subdomain masses m_i .⁷ From Eqs. (36), (21), and (22), we obtain a first-order approximation of the linear decay rate of the r th modal velocity

$$\gamma_r = \frac{2\sqrt{2}}{\pi} \beta \mu_q \quad (37)$$

From Eq. (37), the first-order approximations of the linear decay rates of the modal velocities are identical. Upon examining Eq. (35), three properties are observed.

1) The impulsive damping control algorithm is independent of spacecraft stiffness.

2) The control forces are proportional to the mass in their respective subdomains. This property is attractive in the sense that it confirms the reader's instincts. Indeed, just as it is fundamentally suggested by Newton's laws of motion and Eq. (35), we intuitively recognize that the force required to accelerate an object, or specifically to dampen its motion, is proportional to the object's mass.

3) The impulsive damping control algorithm is decentralized in space; that is, the control force at x_r is obtained by feeding back information and sensor measurements taken at x_r and without regard to other points on the spacecraft.

VI. Impulsive Damping of a Cantilevered Beam

Consider a uniform cantilevered beam. The stiffness operator in Eq. (23) is $T = EI(\partial^4/\partial x^4)$. The cantilevered beam satisfies the boundary conditions $u(0, t) = (\partial/\partial x)u(0, t) = (\partial^2/\partial x^2)u(L, t) = (\partial^3/\partial x^3)u(L, t) = 0$. We let $L = 1$, $\rho = 1$, and $EI = 0.1$ units. The natural frequencies and natural modes of vibration admit closed-form expressions.⁹ Three modes are assumed to significantly contribute to the system's response.

The three lowest natural frequencies are $\omega_1 = 0.35$, $\omega_2 = 2.20$, and $\omega_3 = 6.17$ rad/s. Three control forces are located at $x_1 = 0.33$, $x_2 = 0.67$, and $x_3 = 1.00$. In each case, the beam is excited by an impulse of magnitude 0.1 at $x_0 = 0.75$. Figure 6 shows the free tip response over a 60-s interval. Figures 7, 8, and 9 show the tip response. In each case, we use a rectangular window and a control force level of $\beta m_r = 0.0035$ in Eq. (35). Displacement and velocity deadband levels are 0.06 and 0.03, respectively. Figure 7 has a window size of $T_0 = 4$ s, a displacement gain $\mu_q = 1.4213$, and a velocity gain $\mu_q = 0.70$. Figure 8 has an identical window size but the displacement gain is 1.0824 and the velocity gain is 1.00. The parameters in Fig. 9 are identical to those in Fig. 7 except the window size is extended to 10 s. Figures 7 and 8 demonstrate that control of the structure takes more time as the control gains move higher on the gain constraint curve (Fig. 4). This is dependent on the amount of time associated with $E_1 \cap E_2$. Figures 7 and 9 demonstrate, with a larger window, that the transient standard deviation has more difficulty in adjusting to the transients of the response. The large initial amplitudes bias the approximation and subsequently produce reduced pulse times.

VII. Conclusions

In retrospect, the research community involved in the development of fuel optimal control algorithms for flexible spacecraft has frequently adopted the approach of approximating the associated necessary conditions of optimality. Another approach presented here approximates the solution to the fuel optimal control problem. This approximation is based on inherent properties associated with the exact solution of the harmonic oscillator. Indeed, the near fuel optimal solution approximates impulsive forces by short duration pulses and maximum absolute velocities, and minimum absolute displacements are accurately approximated by transient values of their respective standard deviations. The resulting impulsive damping control algorithms exhibit some distinctly attractive features, as described in the paper.

Acknowledgments

Portions of this investigation were supported by the Mars Mission Research Center under Contract NAGW-1331 and NASA Langley Research Center under Contract NAG-1-977. John L. Meyer is acknowledged for his valuable suggestions and for his generation of the numerical results and Robert Irvine is acknowledged for generating Table 1.

References

- Redding, D. C., and Adams, N. J., "Optimized Rotation-Axis Attitude Maneuver Controller for the Space Shuttle Orbiter," *Journal of Guidance, Control, and Dynamics*, Vol. 10, No. 1, 1987, pp. 4-13.
- Neustadt, L. W., "Minimum Effort Control Systems," *Journal of the Society for Industrial and Applied Mathematics*, Vol. 1, No. 1, 1962.
- Souza, M. L. O., "Exactly Solving the Weighted Time/Fuel Optimal Control of an Undamped Harmonic Oscillator," *Journal of Guidance, Control, and Dynamics*, Vol. 11, No. 6, 1988, pp. 488-494.
- VanderVelde, W. E., and He, J., "Design of Space Structure Control Systems Using On-Off Thrusters," *Journal of Guidance, Control, and Dynamics*, Vol. 6, No. 1, 1983, pp. 53-60.
- Redmond, J., and Silverberg, L., "Fuel Consumption in Optimal Control," *Journal of Guidance, Control, and Dynamics* (to be published).
- Silverberg, L., and Morton, M. H., "On the Nature of Natural Control," *Journal of Vibration, Stress, and Reliability in Design*, Vol. 111, Oct. 1989, pp. 412-422.
- Silverberg, L., Redmond, J., and Weaver, L., "Uniform Damping Control: Discretization and Optimization," *Proceedings of the 7th VPI&SU/AIAA Symposium on Dynamics and Control of Large Structures*, edited by L. Meirovitch, Blacksburg, VA, 1989.
- Foster, L., and Silverberg, L., "On-Off Decentralized Control of Flexible Structures," *Journal of Dynamic Systems, Measurement, and Control*, Vol. 113, March 1991, pp. 41-47.
- Meirovitch, L., *Elements of Vibration Analysis*, McGraw-Hill, New York, 1975.